ARTICLE IN PRESS

Available online at www.sciencedirect.com
SCIENCE DIRECT®

Chemical Physics Letters 418 (2005) 213–218

CHEMICAL PHYSICS LETTERS

www.elsevier.com/locate/cplett

Thermo-mechanical properties of tri-functionally crosslinked liquid single crystal elastomers

Dong-Uk Cho [a,*], Yusril Yusuf [a], P.E. Cladis [b], Helmut R. Brand [c], Heino Finkelmann [d], Shoichi Kai [e,a]

[a] *Department of Applied Quantum Physics and Nuclear Engineering, Graduate School of Engineering, Kyushu University, Fukuoka 812-8581, Japan*
[b] *Advanced Liquid Crystal Technologies, POB 1314, Summit, NJ 07902, USA*
[c] *Theoretische Physik III, Universität Bayreuth, 95440 Bayreuth, Germany*
[d] *Makromolekulare Chemie, Universität Freiburg, 79104 Freiburg, Germany*
[e] *Department of Applied Quantum Physics and Nuclear Engineering, Graduate School of Engineering, Department of Life Engineering, Graduate School of Systems Life Sciences, Kyushu University, Fukuoka 812-8581, Japan*

Received 23 August 2005; in final form 26 October 2005

Abstract

We have investigated thermo-mechanical properties and optical birefringence of the V3 cross-linker liquid single crystal elastomers (V3LSCEs) with different concentrations of the flexible tri-functional cross-linker as a function of temperature. The length of V3LSCEs along the director $\hat{\mathbf{n}}$ shrinks on heating while it expands perpendicular to $\hat{\mathbf{n}}$. Drastic length changes as well as large variations in the optical birefringence, Δn, are observed near T_c. The maximum contraction increases with increasing cross-linking concentration. When the anisotropy of the shape change is plotted as a function of Δn, a linear dependence is observed only deep in the nematic phase for larger cross-linking concentrations.

1. Introduction

Liquid crystal elastomers (LCEs) continue to fascinate scientists with their large thermo-mechanical and electro-mechanical properties [1–17]. LCEs have an axis of anisotropy [1–5]. In monodomain nematic LCEs, liquid single crystal elastomers (LSCEs), the director axis of the mesogenic units is macroscopically uniformly aligned. The result is a transparent material with anisotropic optical, mechanical, and electrical properties [2–6]. At the nematic to isotropic phase transition these LSCEs shows a significant shape change. This thermo-mechanical deformation of LSCEs has received considerable attention as a candidate for soft artificial muscles [5–10]. Recently, swollen LCEs have also been demonstrated to show substantial electro-mechanical effects [17,18].

Basically LSCEs consist of the cross-linked polymer chain networks and the liquid crystalline ordering of side chain mesogenic groups [2–6]. The network was synthesized in two steps by addition of bi-functional cross-linking agents to the polymer chains, with the second cross-linking step being carried out under the influence of a large enough strain giving rise to a uniform director orientation denoted by a unit pseudo-vector $\hat{\mathbf{n}}$ [2,5].

Thermo-mechanical properties of bi-functional cross-linking LSCEs have been investigated in detail [1–4,9–16] where a spontaneous shape change as well as changes in the optical birefringence were observed in the vicinity of the apparent nematic–isotropic transition temperature, T_c. The change of shape does not occur just at the transition, but continues to lower temperatures as the nematic order gets larger and the chains become more anisotropic.

* Corresponding author. Fax: +81 92 642 3820.
E-mail addresses: cho@athena.ap.kyushu-u.ac.jp (D.-U. Cho), kaitap@mbox.nc.kyushu-u.ac.jp (S. Kai).

0009-2614/$ - see front matter © 2005 Elsevier B.V. All rights reserved.
doi:10.1016/j.cplett.2005.10.123

The orientational order of side chain mesogenic groups inside LSCE influences the polymer chain shape. On heating, chain shape changes induce the shape change of the cross-linked polymer chain network as a whole. The shrinkage parallel to $\hat{\mathbf{n}}$ and the expansion perpendicular to $\hat{\mathbf{n}}$ in length on heating indicate the anisotropic behavior of LSCE.

Here we investigate how the shape-changing and optical properties of LSCEs are affected when the cross-linking agent is tri-functional instead of bi-functional. The tri-functional, flexible cross-linker is used to minimize effects of the cross-linker on the isotropic to nematic phase transformation (compare, e.g., [19]). While a rigid bi-functional cross-linker causes a broad transition, the transition with the tri-functional cross-linker is within a relatively narrow temperature regime.

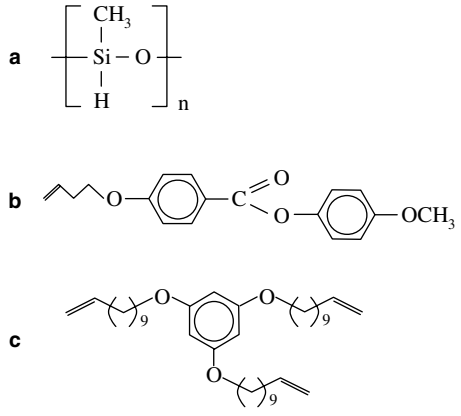

Fig. 1. The chemical structures of the compounds prepared for the V3LSCEs. (a) The methylsiloxane monomer backbone. (b) The mesogenic biphenyl side chain. (c) The tri-functional cross-linker.

2. Experimental

The V3LSCEs materials studied here were originally invented and developed by one of present authors (H. F.). The chemical structures of the V3LSCE are shown in Fig. 1. The polymer backbone is a poly-methylhydrosiloxane. The pendant mesogenic groups are 4-(3-butenoxy) benzoic acid-(4-methoxy) phenyl attached to the backbone via a hydrosilation reaction. The networks are chemically crosslinked with the V3 crosslinker 1,3,5-tris-undec-10-enoxy-benzene. The cross-linking concentrations are 3.3 mol% (V3LSCE-3), 5 mol% (V3LSCE-5) and 7 mol% (V3LSCE-7).

Two types of rectangular V3LSCEs samples with different bulk director orientation with respect to $\hat{\mathbf{n}}$ were investigated. One is obtained by slicing parallel to $\hat{\mathbf{n}}$ (planar sample) and the other is obtained by slicing perpendicular to $\hat{\mathbf{n}}$ (homeotropic sample); both were prepared to measure shape changes. The thickness of the samples is $\sim$400 μm and the area is $\sim 0.7 \times 0.5$ mm. The sample is observed by a microscope (Nikon) equipped with a hot stage (Mettler Toledo FP90 Central Processor) as a temperature controller. The image of each temperature photographed during the heating and cooling processes with a range between 30 and 100 °C and the scan rate of temperature is about 0.5 K/min.

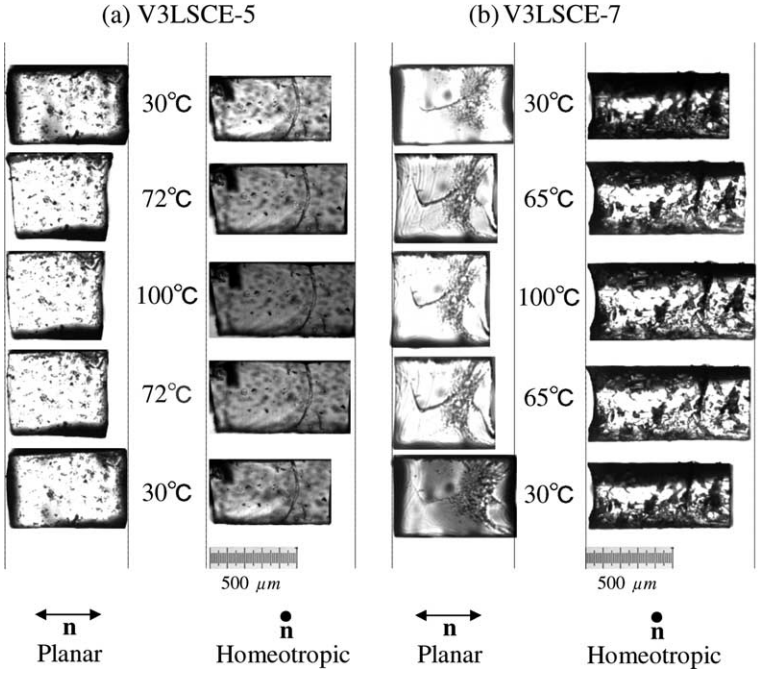

Fig. 2. Thermo-mechanical effect induced shape changes of V3LSCE-5 (a) and V3LSCE-7 (b), for planar and homeotropic samples. The scan rate of temperature was 0.5 K/min. V3LSCEs shrink $\|\hat{\mathbf{n}}$ on heating and expand on cooling. In contrast, V3LSCEs expand $\perp \hat{\mathbf{n}}$ on heating and shrink on cooling.

For the birefringence measurements we prepared samples of $\sim 1.5 \times 2.0$ mm area and ~ 70 μm thickness. The intensity of transmitted light during the heating process is observed using the polarizing microscope equipped with a hot stage as a temperature controller and a He–Ne laser as a light source.

3. Results and discussion

The anisotropic thermo-mechanical effects for V3LSCE-5 and V3LSCE-7 samples during the heating and the cooling processes are shown in Fig. 2. When increasing the temperature the planar samples shrink parallel to $\hat{\mathbf{n}}(\hat{x})$ and expand

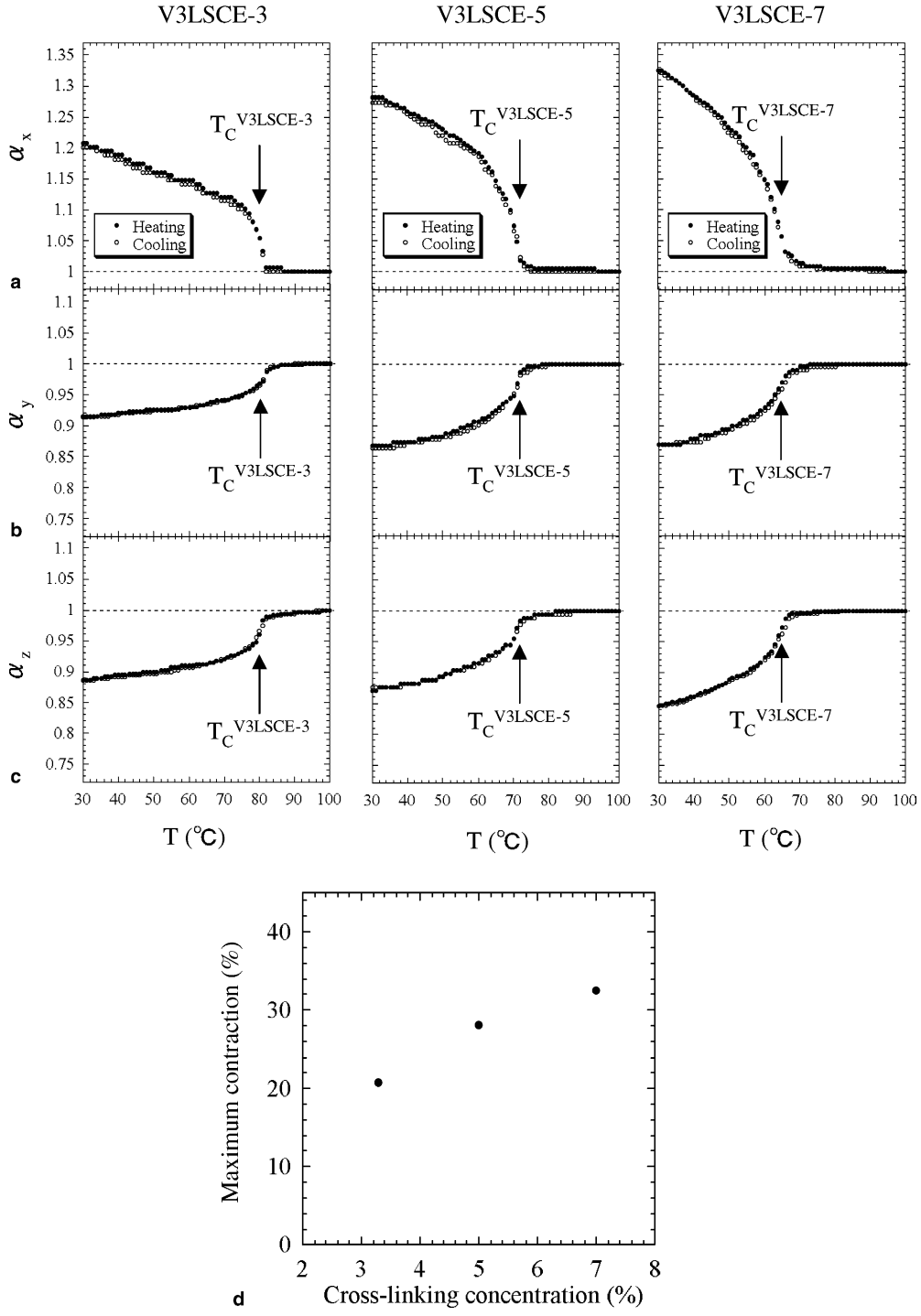

Fig. 3. Temperature dependence of the relative length changes, $\alpha_i(T)$, for V3LSCE-3, V3LSCE-5 and V3LSCE-7 samples during the heating (●) and the cooling (○) processes. (a) $\alpha_x \| \hat{\mathbf{n}}$, (b) $\alpha_y \perp \hat{\mathbf{n}}$ and (c) $\alpha_z \perp \hat{\mathbf{n}}$. Drastic shape changes are observed near $T_c(T_c^{V3LSCE-3} \sim 80\ ^\circ C, T_c^{V3LSCE-5} \sim 72\ ^\circ C$, and $T_c^{V3LSCE-7} \sim 65\ ^\circ C)$. No hysteresis is observed on heating and cooling. (d) The dependence of the maximum length change $\| \hat{\mathbf{n}}$ on the concentration of cross-linking of V3LSCEs in the isotropic phase ($T = 100\ ^\circ C$) is plotted. The maximum contraction increases with increasing the cross-linking concentration.

perpendicular to $\hat{\mathbf{n}}(\hat{y})$. In contrast, for the homeotropic samples, both directions perpendicular to $\hat{\mathbf{n}}$ expand. After cooling, all samples return to their original shape.

Mesogenic side chain groups in the polymer network are aligned on average parallel to an externally determined $\hat{\mathbf{n}}$ in a two-step synthesis [3]. When heating, gradually thermal fluctuations of mesogenic molecules induce orientation changes of mesogenic side chains, i.e., they decrease the nematic order, and give rise to shape changes of the cross-linked polymer chain network and to the resulting mechanical deformations of V3LSCE samples, namely a shrinkage parallel to $\hat{\mathbf{n}}$ and an expansion in the direction perpendicular to $\hat{\mathbf{n}}$.

To quantify the volume changes of V3LSCEs, we define the relative length changes of planar and homeotropic samples as a function of temperature, $\alpha_l(T)$, as the ratio of expansion/shrinkage length to the initial length in the isotropic phase ($T = 100\,^{\circ}\mathrm{C}$). Length measurements were made in the middle of each edge far from other edges. The relative error was $\sim\pm 1\%$ due to the pixel size of the photo micrograph.

Fig. 3 shows the relative length changes of V3LSCEs parallel to $\hat{\mathbf{n}}(\hat{x})$ and perpendicular to $\hat{\mathbf{n}}(\hat{y}$ and $\hat{z})$ as a function of temperature. Increasing temperature, all samples monotonically shrank parallel to $\hat{\mathbf{n}}(\hat{x})$ (Fig. 3a) with a somewhat faster decrease in the vicinity of $T_c^{\text{V3LSCE-3}} \sim 80\,^{\circ}\mathrm{C}$, $T_c^{\text{V3LSCE-5}} \sim 72\,^{\circ}\mathrm{C}$, and $T_c^{\text{V3LSCE-7}} \sim 65\,^{\circ}\mathrm{C}$ for the V3LSCE-3, V3LSCE-5 and V3LSCE-7 samples, respectively. V3LSCE reaches a maximum shrinkage of about 20% for V3LSCE-3, 28% for V3LSCE-5, and 32% for V3LSCE-7. In contrast, V3LSCEs monotonically expand in the direction perpendicular to $\hat{\mathbf{n}}(\hat{y}$ and $\hat{z})$ (Fig. 3b and c) on heating and reach a maximum expansion of about 12% for V3LSCE-3, 14% for V3LSCE-5, and 16% for V3LSCE-7.

The phase behavior of the liquid crystal elastomers depends on the cross-linking conditions [3,20]. The V3LSCEs materials studied here have been crosslinked in the nematic phase. The presence of a higher density of cross-linking points appears to reduce the degree of nematic order by increasing the general disorder and/or by reducing – due to the higher density of cross-linking points – the nematogenic tendencies. Increasing the cross-linking concentration will thus favor the isotropic state of the system and reduce the nematic-isotropic phase transition temperature T_c as observed in V3LSCE samples.

We plot the maximum contraction of V3LSCEs with different cross-linking concentrations in Fig. 3d. The maximum contraction (in the direction parallel to $\hat{\mathbf{n}}$) increases slightly with increasing cross-linking concentrations. These results strongly suggest that the denser cross-linking lead to stronger rubber elasticity and a larger length contraction.

Fig. 4 shows the measured optical birefringence, Δn, of the V3LSCEs as a function of temperature. In a previous communication [11], we have introduced the experimental technique for birefringence measurements. The maximum value of Δn is about 0.12 for V3LSCE-3, 0.14 for V3LSCE-5 and 0.13 for V3LSCE-7 at low temperatures (in the nematic phase). Significant changes of Δn are observed near $T_c^{\text{V3LSCE-3}} \sim 80\,^{\circ}\mathrm{C}$, $T_c^{\text{V3LSCE-5}} \sim 72\,^{\circ}\mathrm{C}$, and $T_c^{\text{V3LSCE-7}} \sim 65\,^{\circ}\mathrm{C}$ for V3LSCE-3, V3LSCE-5 and V3LSCE-7, respectively. These temperatures agree with the results of length changes at the apparent nematic-isotropic phase transition temperature (Fig. 3a).

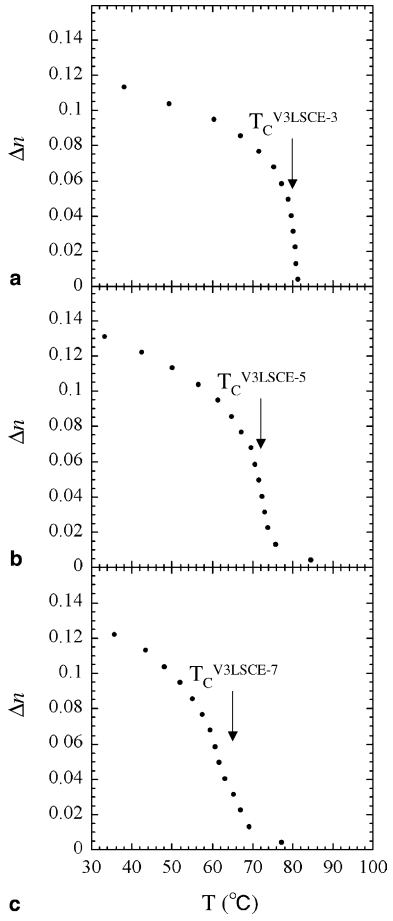

Fig. 4. Optical birefringence, Δn, for V3LSCE-3 (a), V3LSCE-5 (b) and V3LSCE-7 (c) as a function of temperature.

Due to frozen-in nematic order in the vicinity of the cross-linking points, there is a finite value Δn above T_c for the higher cross-linking concentrations, i.e., the V3LSCE-5 and V3LSCE-7 samples. Just above T_c, local nematic order inside the network cannot change into the isotropic phase. This fact is a consequence of 'frozen in' nematic order [21], an important feature of LSCEs. This is also the reason why smooth length changes are observed just above T_c for V3LSCE-5 and V3LSCE-7 (Fig. 3a).

In [22] for nematic polydomain LCEs and, subsequently, for monodomain LCEs [2,3] it has been demonstrated that one can either use the optical birefringence, Δn, or equivalently the strain parallel to the director field, $\hat{\mathbf{n}}$, to characterize the degree of nematic order. Well inside the nematic phase a linear relation between Δn and the strain was shown to result [22,2,3].

Since we have measured for the present work the relative length changes parallel to the director as well as in the two

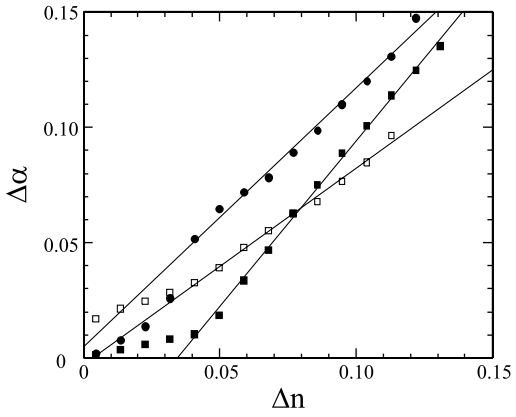

Fig. 5. The shape anisotropy, $\Delta\alpha$, is plotted as a function of the optical birefringence, Δn, for samples with the three crosslinking densities studied here. ● Corresponds to the data points of the sample with 7% crosslinking density, filled squares to 5% and □ to 3.3% cross-linking density. The straight lines plotted are obtained as a fit to the data well inside the nematic phase, that is with a $\Delta n \geqslant 0.04$. The direct proportionality shows that Δn as well as the shape anisotropy, $\Delta\alpha$, can be used equally well to describe the degree of order in a nematic LSCE.

directions perpendicular to the director, we introduce here the shape anisotropy $\Delta\alpha$ to characterize the mechanical deformations and to make optimum use of the data.

We define the shape anisotropy, $\Delta\alpha$, as follows:

$$\Delta\alpha = \frac{\alpha_x - [\alpha_y + \alpha_z]/2}{\alpha_x + \alpha_y + \alpha_z}. \quad (1)$$

It is straightforward to show that for linear elasticity and assuming incompressibility, $\Delta\alpha$ and the length change parallel to the director are completely equivalent. Accordingly, we plotted in Fig. 5 the shape anisotropy, $\Delta\alpha$, as a function of the optical birefringence, Δn.

We see from Fig. 5 that we also find for LSCEs using the tri-functional cross-linker V3 a linear relation between the shape anisotropy and the optical birefringence well inside the nematic phase. This is in close agreement with the previous plots displaying Δn versus the length change obtained for bi-functional cross-linkers [22,2,3].

We note that the finite value for the sample with a cross-linking density of 3.3% for small values of Δn is most likely due to the fact that this sample was not completely of monodomain character.

We close this section by discussing the volume changes of the samples as a function of temperature. The volume of the three samples V3LSCE-3, V3LSCE-5 and V3LSCE-7 well inside the isotropic phase at $T = 100$ °C increased by about 2% compared to the initial volume well inside the nematic phase. Within the error bar of our measurements, the maximum degree of volume expansion is independent of the cross-linking concentration.

4. Conclusion

We have discussed shape changes and optical birefringence of V3LSCEs with different cross-linking concentrations as a function of temperature. While a rigid bi-functional cross-linker causes a broad transition, the transition with the tri-functional cross-linker is within a relatively narrow temperature regime. We found that the maximum contraction of V3LSCEs increases with increasing cross-linking concentrations. From this result, we conclude that denser cross-linking of the V3LSCEs decreases thermal fluctuations of liquid crystalline mesogenic side chain molecules inside the polymer networks. That is, denser cross-linking leads to higher elasticity and to larger length contraction. Furthermore, we have shown that the shape anisotropy, $\Delta\alpha$, is a suitable quantity to characterize the degree of nematic order in LSCEs well inside the nematic phase using a tri-functional cross-linker: when the anisotropy of the shape change, $\Delta\alpha$, is plotted as a function of Δn, a linear dependence is observed even deep in the nematic phase for the larger cross-linking concentrations, in contrast to previous work using bi-functional cross-linkers in monodomain LSCEs. The maximum volume expansion is about 2%, a value that is independent of the cross-linking concentration.

Acknowledgments

We thank Elke Stibal-Fischer for sending us the samples used in these measurements. This work is partially supported by the Japan-Germany Scientific Cooperative Program of the Japan Society for the Promotion of Science and the Deutsche Forschungsgemeinschaft, and the Grant for Scientific Research sponsored by the Japan Society for the Promotion of Science. P.E.C thanks the Japan Society for the Promotion of Science for the award of a JSPS Research Prize that enabled this collaboration. H.R.B. thanks the Deutsche Forschungsgemeinschaft for partial support of his work through Sonderforschungsbereich 481 'Komplexe Polymer- und Hybridmaterialien in inneren und äußeren Feldern. Y.Y. thanks the Research Fellowships of the Japan Society for Promotion of Science (JSPS).

References

[1] H. Finkelmann, H.J. Kock, G. Rehage, Makromol. Chem. Rapid Commun. 2 (4) (1981) 317.
[2] J. Kupfer, H. Finkelmann, Makromol. Chem. Rapid Commun. 12 (1991) 717.
[3] J. Kupfer, H. Finkelmann, Makromol. Chem. Phys. 195 (1994) 1353.
[4] F.J. Davis, G.R. Mitchell, Polymer 37 (1996) 1347.
[5] I. Kundler, H. Finkelmann, Macromol. Chem. Phys. 199 (1998) 677.
[6] M. Warner, E.M. Terentjev, Liquid Crystal Elastomers, Clarendon Press, Oxford, 2003.
[7] P.G. de Gennes, M. Hubert, R. Kant, Macromol. Symp. 113 (1997) 39.
[8] M. Hubert, R. Kant, P.G. de Gennes, J. Phys. I France 7 (1997) 909.
[9] Y. Yusuf, P.E. Cladis, H.R. Brand, H. Finkelmann, S. Kai, Chem. Phys. Lett. 389 (2004) 443.
[10] Y. Yusuf, Y. Ono, Y. Sumisaki, P.E. Cladis, H.R. Brand, H. Finkelmann, S. Kai, Phys. Rev. E 69 (2004) 021710.
[11] Y. Yusuf, Y. Sumisaki, S. Kai, Chem. Phys. Lett. 382 (2003) 198.
[12] S.M. Clarke, E.M. Terentjev, I. Kundler, H. Finkelmann, Macromolecules 31 (15) (1998) 4862.

[13] M.C-. Lopez, H. Finkelmann, P.P-. Muhoray, M. Shelley, Nature Materials 3 (5) (2004) 307.
[14] A.R. Tajbakhsh, E.M. Terentjev, Eur. Phys. J.E 6 (2001) 181.
[15] D.L. Thomsen III, P. Keller, J. Naciri, R. Pink, H. Jeon, D. Shenoy, B.R. Ratna, Macromolecules 34 (2001) 5868.
[16] P.E. Cladis, in: P. Ehrhard, D.S. Riley, P.H. Steen (Eds.), Interactive Dynamics of Convection and Solidification, Kluwer, Dordrecht, 2001, p. 123.
[17] J.H. Huh, J. Xin, Y. Yusuf, S. Kai, J. Phys. Soc. Jpn. 74 (2005) 242.
[18] Y. Yusuf, J.H. Huh, P.E. Cladis, H.R. Brand, H. Finkelmann, S. Kai, Phys. Rev. 71 (2005) 061702.
[19] A. Greve, H. Finkelmann, Macromol. Chem. Phys. 202 (2001) 2926.
[20] M. Warner, K.P. Gelling, T.A. Vilgis, J. Chem. Phys. 88 (1988) 4008.
[21] H.R. Brand, K. Kawasaki, Macromol. Rapid Comm. 15 (1994) 251.
[22] W. Kaufhold, H. Finkelmann, H.R. Brand, Makromol. Chem. 192 (1991) 2555.